This paper is published as part of a *Dalton Transactions* themed issue on:

N-Heterocyclic Carbenes

Guest Editor Ekkehardt Hahn

Westfälische Wilhelms-Universität, Münster, Germany

Published in issue 35, 2009 of *Dalton Transactions*

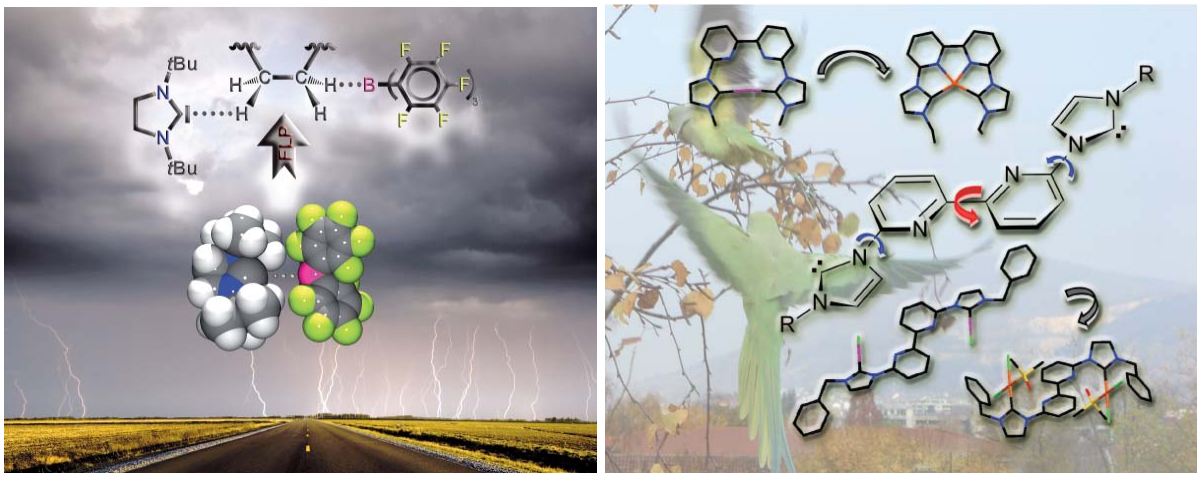

Images reproduced with permission of Matthias Tamm (left) and Doris Kunz (right)

Articles published in this issue include:

PERSPECTIVES:

HOT PAPERS:

Visit the *Dalton Transactions* website for more cutting-edge inorganic and organometallic research
www.rsc.org/dalton

Syntheses and catalytic activities of pseudo-pincer and CSC pincer-type Pd(II) complexes derived from benzannulated N-heterocyclic carbenes†

Han Vinh Huynh,* Dan Yuan and Yuan Han

Received 20th April 2009, Accepted 22nd July 2009
First published as an Advance Article on the web 31st July 2009
DOI: 10.1039/b907887h

Three new dibenzimidazolium salts bearing thioether (**B**·2HBr, **B**·2HNO$_3$) and sulfoxide (**C**·2HBr) containing bridges have been synthesized as sulfur-functionalized dicarbene precursors. Palladation of **B**·2HBr and **C**·2HBr afforded two new pseudo-pincer complexes *cis*-[PdBr$_2$(**B**-κ^2*C*)] (**1**) and *cis*-[PdBr$_2$(**C**-κ^2*C*)] (**2**), in which the sulfur-donor remains pendant. Reaction of precursor **B**·2HNO$_3$ in the presence of 1 equiv of KBr, on the other hand, yields the first CSC-Pd(II) pincer complex [PdBr(**B**-κ^3*CSC*)]NO$_3$ (**3**) bearing two carbene moieties. All three complexes have been fully characterized by multinuclei NMR spectroscopies, ESI mass spectrometry and X-ray diffraction analysis. Their catalytic activities in the Mizoroki–Heck reaction have been evaluated as well.

Introduction

N-heterocyclic carbenes (NHCs) are powerful σ-donors that have become standard ligands in organometallic chemistry and catalysis due to their stabilizing properties and ease of preparation.[1] An additional advantage is that they can be modified in many ways, which also allows for a straightforward donor-functionalization[2] giving access to ditopic and pincer-type ligands, the complexes of which have found widespread applications in catalytic processes.[3] Heteroatom-NHC pincers have been generally prepared by combining one or two NHC moieties with nitrogen, phosphorus or oxygen donors, whereas sulfur-containing analogues are very rare, possibly due to lack of suitable synthetic methodologies.[4] To the best of our knowledge, only two examples of dithiolato[5,6] SCS NHC-based pincer-ligands have been reported so far. CSC pincer ligands based on NHCs are on the other hand unknown. Furthermore, most known pincer systems contain a rather rigid structure, which is intended to yield increased complex stability. On the other hand, a more flexible ligand backbone would allow a more subtle interplay between lability and stability, which may be beneficial for certain types of catalytic applications. In relation to our research on less explored sulfur-functionalized NHCs, we have recently reported on complexes bearing ditopic and hemilabile thioether-[7] and thiophene-[8] NHC ligands. As an extension of our work in this area, we herein report on the syntheses, structural characterization and catalytic activities of the first CSC-pincer-type Pd(II) complex and two of its "quasi-pincer" analogues, in which the flexible and soft sulfur moiety remains pendant.

Results and discussion

Sulfur-functionalized dibenzimidazolium salts

The preparation of thioether- and sulfoxide-bridged dibenzimidazolium salts as precursors to CSC NHC-based pincer ligands is summarized in Scheme 1. The reaction of benzylbenzimidazole with neat dibromoethane afforded 1-benzyl-3-bromoethylbenzimidazolium bromide **A** in a yield of 92%. Salt **A** is soluble in dichloromethane, and thus can be easily separated from small amounts of the ethylene bridged dibenzimidazolium salt that has formed as a by-product. The formation of **A** is supported by a base peak in the ESI mass spectrum at $m/z = 316$ for the molecular cation [M – Br]$^+$. Furthermore, its ^{1}H NMR spectrum shows a downfield shift at 10.12 ppm characteristic for the NCHN proton in azolium salts and two triplets at 5.03 and 4.08 ppm

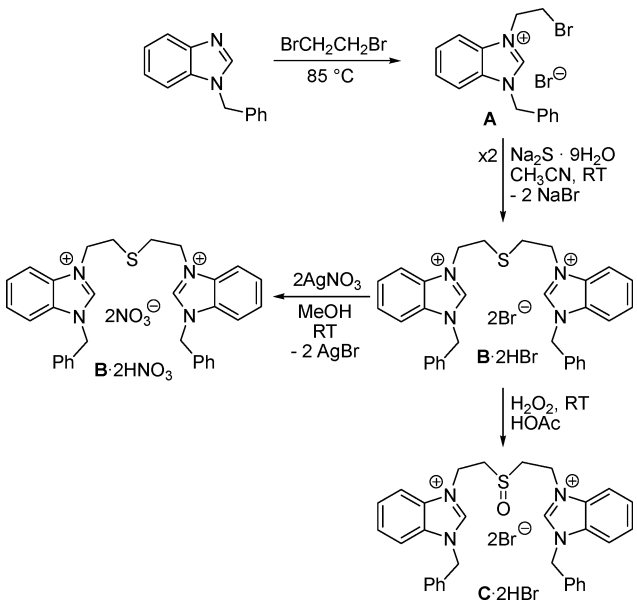

Scheme 1 Synthesis of benzimidazolium salts.

Department of Chemistry, 3 Science Drive 3, National University of Singapore, Singapore 117543. E-mail: chmhhv@nus.edu.sg; Fax: +65 67791691; Tel: +65 65162670

† CCDC reference numbers 728535 (**B**·2HBr·0.8H$_2$O), 728532 (**1**), 728533 (**2**·0.5DMF) and 728534 (**3**). For crystallographic data in CIF or other electronic format see DOI: 10.1039/b907887h

with vicinal coupling constant ^3J(H-H) = 5.8 Hz assignable to the two inequivalent methylene groups of the bromoethylene *N*-substituent. The benzylic protons on the other hand resonate as a singlet at 5.85 ppm.

Two equiv of **A** can subsequently undergo nucleophilic substitution with Na_2S to form the thioether-bridged dibenzimidazolium dibromide **B**·2HBr, which was isolated as an off-white powder in 87% yield. Compared to precursor **A**, the ^{1}H NMR signals do not change significantly upon thioether-formation. Only a slight upfield shift was observed for the methylene groups adjacent to the sulfur atom. Stronger evidence for the identity of **B**·2HBr was provided by a base peak in the ESI mass spectrum at m/z = 252 for the molecular dication $[M - 2Br]^{2+}$ and a less intense peak at m/z = 585 for the mono-cation $[M - Br]^+$. Single crystals of **B**·2HBr·0.8H_2O were obtained by slow evaporation of a concentrated methanol solution and subjected to single-crystal X-ray diffraction. Fig. 1 depicting its molecular structure along with the crystallographic numbering scheme, shows the expected connectivity and the presence of the desired thioether function bridging the two cationic benzimidazolium fragments. All bond parameters are in the expected range and do not require further comments.

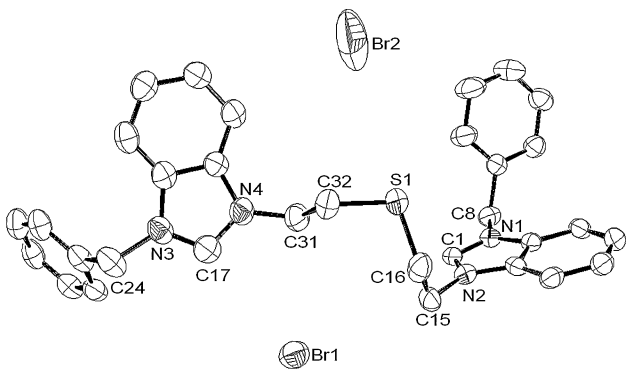

Fig. 1 Molecular structure of **B**·2HBr·0.8H_2O showing 50% probability ellipsoids; hydrogen atoms and solvent molecules are omitted for clarity. Selected bond lengths (Å) and angles (°): N3–C24 1.505(9), N3–C17 1.333(10), N4–C17 1.343(9), N4–C31 1.489(9), C31–C32 1.525(10), C32–S1 1.819(7), S1–C16 1.842(7), C16–C15 1.513(11), N2–C15 1.493(8), N2–C1 1.339(8), C1–N1 1.333(8), N1–C8 1.489(8); N3–C17–N4 110.9(7), N2–C1–N1 110.1(5).

Anion exchange occurs smoothly by reacting **B**·2HBr with two equiv of $AgNO_3$ affording **B**·2HNO_3 with precipitation of AgBr. Again, ESI MS proved useful in the characterization of the product with a base peak at m/z = 252 assignable for the $[M - 2NO_3]^{2+}$ dication and a less intense peak at m/z = 566 for the mono-cation $[M - NO_3]^+$. In addition, the sulfoxide-bridged dibenzimidazolium salt **C**·2HBr was prepared by oxidation of the thioether **B**·2HBr with three equiv of H_2O_2 in acetic acid. Successful oxidation was indicated by a base peak at m/z = 260 for the dication $[M - 2Br]^{2+}$ and a smaller one centered at m/z = 601 for the mono-cation $[M - Br]^+$. Upon formation of the sulfoxide function, all protons of the bridge and their respective carbon atoms shift downfield, which is in line with the increased $-I$-effect of the resulting sulfoxide group. Furthermore, the α-protons also become diastereotopic due to the reduced inversion of the oxidized and pyramidal sulfur atom. All other groups remain largely unaffected by this conversion and their chemical shifts show little changes. The benzimidazolium salts **A**, **B**·2HBr, **B**·2HNO_3 and **C**·2HBr are all non-hygroscopic powders and can be easily handled in air.

Palladium(II) complexes

The suitability of the proligands **B**·2HBr, **C**·2HBr and **B**·2HNO_3 to form Pd(II)-complexes was probed by reacting them with $Pd(OAc)_2$ in DMSO at elevated temperatures. The reaction sequences are summarized in Scheme 2. Palladation of **B**·2HBr leads to the pseudo-pincer dicarbene Pd(II) complex *cis*-[$PdBr_2$(**B**-κ^2C)] (**1**), in which the thioether function remains pendant. The neutral complex was isolated as a stable yellow solid soluble in CH_2Cl_2, $CHCl_3$, DMSO, and DMF, but insoluble in less polar solvents such as THF, diethyl ether and hexane. The formation of a Pd(II) carbene complex is supported by positive mode ESI mass spectrometry, which shows a base peak at m/z = 689 for the $[M - Br]^+$ complex fragment. Besides, the disappearance of the NCHN signal in the ^{1}H NMR spectrum characteristic for **B**·2HBr, the metallation results in diastereotopy of the benzylic protons with chemical shifts of 6.35 and 5.30 ppm, respectively, with geminal coupling constants of 16.4 Hz. Likewise, the methylene protons of the bridge adjacent to the nitrogen also give rise to two signals at 5.84 and 4.85 ppm. The methylene groups adjacent to the sulfur atom, on the other hand, resonate as one multiplet at 3.50 ppm, which indicates a certain degree of rotational freedom in line with a pendant sulfur function. This is further supported by the ^{13}C NMR signal for carbene carbon found at 175.2 ppm. This chemical shift corroborates a *cis*-arrangement of the two benzimidazolin-2-ylidene donors disfavoring coordination of the thioether bridge in a square planar complex.[9]

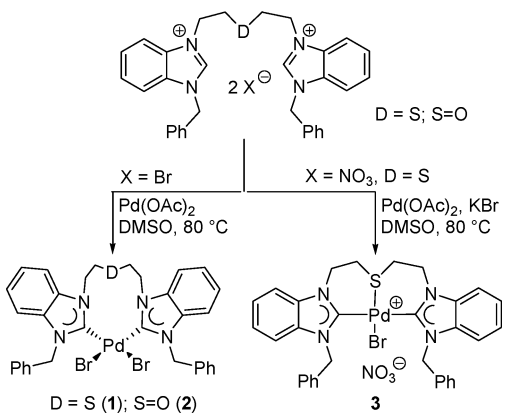

Scheme 2 Synthesis of pseudo-pincer complexes **1**, **2** and CSC pincer complex **3**.

The identity of **1** as a pseudo-pincer was finally confirmed by X-ray diffraction analysis on a single crystal obtained from slow vapour diffusion of diethyl ether into a concentrated DMF solution. Fig. 2 depicts the molecular structure, and selected crystallographic data are listed in Table 3. As found in solution, the dicarbene ligand **B** coordinates the palladium(II) center in a *cis*-chelating fashion, which results in a ten-membered metallacycle. The pendant sulfur atom is oriented "exo" with respect to the metal center and points away from the coordination plane. A similar arrangement has been observed for a related Pd(II) quasi-pincer complex of an ether-bridged diimidazolin-2-ylidene ligand.[10] The

Table 1 Mizoroki–Heck coupling reactions[a] catalyzed by complexes **1-3**

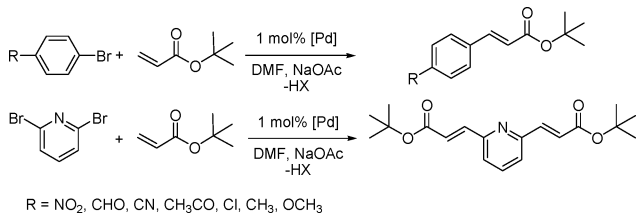

R = NO_2, CHO, CN, CH_3CO, Cl, CH_3, OCH_3

Entry	Catalyst	Aryl halide	*t* [h]	Temp [°C]	Yield [%][b]
1	**1**	4-bromo-1-nitrobenzene	24	120	>99
2	**2**	4-bromo-1-nitrobenzene	24	120	>99
3	**3**	4-bromo-1-nitrobenzene	24	120	>99
4	**1**	4-bromobenzaldehyde	24	120	>99
5	**2**	4-bromobenzaldehyde	24	120	>99
6	**3**	4-bromobenzaldehyde	24	120	>99
7	**1**	4-bromobenzonitrile	24	120	>99
8	**2**	4-bromobenzonitrile	24	120	>99
9	**3**	4-bromobenzonitrile	24	120	>99
10	**1**	4-bromoacetophenone	24	120	>99
11	**2**	4-bromoacetophenone	24	120	>99
12	**3**	4-bromoacetophenone	24	120	>99
13	**1**	2,6-dibromopyridine	24	120	>99
14	**2**	2,6-dibromopyridine	24	120	>99
15	**3**	2,6-dibromopyridine	24	120	>99
16	**1**	1-bromo-4-chlorobenzene	24	120	50
17	**2**	1-bromo-4-chlorobenzene	24	120	58
18	**3**	1-bromo-4-chlorobenzene	24	120	45
19	**1**	4-bromotoluene	24	140	53[c]
20	**2**	4-bromotoluene	24	140	52[c]
21	**3**	4-bromotoluene	24	140	47[c]
22	**1**	4-bromoanisole	24	140	41[c]
23	**2**	4-bromoanisole	24	140	35[c]
24	**3**	4-bromoanisole	24	140	51[c]

[a] Reaction conditions: 1 mmol of aryl halide (0.5 mmol of 2,6-dibromopyridine); 1.4 mmol of *tert*-butyl acrylate; 3 ml of DMF; 1.5 mmol of NaOAc; 1 mol% of [Pd]. [b] Yields were determined by ^{1}H NMR spectroscopy for an average of two runs. [c] With addition of 1.5 equiv of $[N(n\text{-}C_4H_9)_4]Br$.

Table 2 Mizoroki–Heck coupling reactions[a] catalyzed by complex **3**

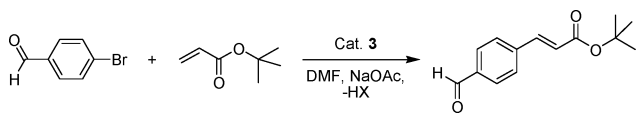

Entry	[Pd] [mol%]	*t* [h]	Temp [°C]	Yield [%][b]	TON
1	0.2	24	120	>99	500
2	0.02	24	120	>99	5000
3	0.002	24	120	>99	50 000
4	0.001	48	120	>99	100 000
5	0.0002	72	120	36	180 000

[a] Reaction conditions: 1 mmol of 4-bromobenzaldehyde; 1.4 mmol of *tert*-butyl acrylate; 3 ml of DMF; 1.5 mmol of NaOAc. [b] Yields were determined by ^{1}H NMR spectroscopy for an average of two runs.

two remaining coordination sites in the square planar complex are taken up by two bromo ligands. The two carbene planes adopt an angle of 80° to each other. Surprisingly, the amount by which the two carbene planes deviate from the PdC_2Br_2 coordination plane is with values of 82° and 71° quite different. At this point this difference can only be ascribed to crystal packing effects, since other interactions could not be discerned. The Pd–C bonds of

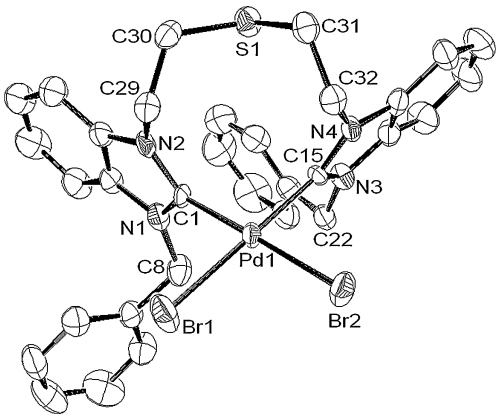

Fig. 2 Molecular structure of pseudo-pincer complex **1** showing 50% probability ellipsoids; hydrogen atoms are omitted for clarity. Selected bond lengths (Å) and angles (°): Pd1–C1 1.951(7), Pd1–C15 1.984(6), Pd1–Br1 2.4684(10), Pd1–Br2 2.4792(9), N1–C8 1.451(11), N1–C1 1.368(10), N2–C1 1.357(10), N2–C29 1.462(10), N3–C15 1.348(9), N3–C22 1.474(10), N4–C32 1.452(10), N4–C15 1.349(9), S1–C30 1.799(8), S1–C31 1.812(8); C1–Pd1–Br1 84.7(2), C1–Pd1–C15 94.5(3), C15–Pd1–Br2 87.8(2), Br1–Pd1–Br2 93.06(4), C15–Pd1–Br1 178.8(2), C1–Pd1–Br2 176.8(2), N1–C1–N2 104.7(6), N3–C15–N4 105.5(6); PdC_2Br_2/NHC dihedral angle 82° and 71°; inter-NHC angle 80°.

1.951(7) and 1.984(6) Å as well as the Pd–Br bonds amounting to 2.4684(10) and 2.4792(9) Å are comparable to those observed for the only other structurally characterized dibenzimidazolin-2-ylidene- dibromo-palladium(II) complex.[11]

The reaction of precursor **C**·2HBr gave similar results and an analogous pseudo-pincer complex *cis*-[$PdBr_2$(**C**-κ^2C)] (**2**) was obtained, which is indicated by a base peak at $m/z = 705$ for the $[M - Br]^+$ ion in the positive mode ESI mass spectrum. Complex **2** dissolves sparingly in acetone and CH_3CN, but shows good solubility in DMSO and DMF. Compared to the ^{1}H NMR spectrum of its ligand precursor **C**·2HBr, in which only the methylene protons adjacent to the sulfoxide group are diastereotopic (*vide supra*), all three methylene groups of the ligand **C** split into six separate signals in accord with an AB coupling pattern upon complex formation. Furthermore, the carbene donors of **2** resonate slightly highfield from those in complex **1** at 173.8 ppm, again indicating a *cis*-arrangement of the benzannulated carbene moieties. The proposed structure was finally confirmed by an X-ray diffraction study on crystals obtained by diffusion of diethyl ether into a DMF solution of **2**. The molecular structure depicted in Fig. 3 is similar to that of complex **1** and features a *cis*-chelating dicarbene and two bromo ligands coordinating the palladium center in a square planar fashion. The resulting 10-membered metallacycle contains the pendant sulfoxide group, which points away from the coordination plane. Similar to **1**, the two carbene planes adopt an angle of 76° relative to each other. Their dihedral angles of 84° and 81° with respect to the PdC_2Br_2 coordination plane fall, in contrast to those in **1**, in a narrow range. All other bond parameters are unexceptional and do not require further comments.

In an attempt to overcome the formation of pseudo-pincer complexes and to enforce a CSC-pincer-type coordination mode of ligand **B**, we substituted the ligand precursor **B**·2HBr with **B**·$2HNO_3$. The latter only contains weakly coordinating counteranions, which should facilitate binding of the soft thioether

Table 3 Selected X-ray crystallographic data for the dibenzimidazolium salt **B**·2HBr·0.8H_2O and the complexes **1**, **2**·0.5DMF and **3**

	B·2HBr·0.8H_2O	**1**	**2**·0.5DMF	**3**
Formula	$C_{32}H_{32}Br2N_4S·0.8H_2O$	$C_{32}H_{30}Br_2N_4PdS$	$C_{32}H_{30}Br_2N_4OPdS·0.5C_3H_7NO$	$C_{32}H_{30}BrN_5O_3PdS$
Formula weight	678.91	768.88	821.43	750.98
Color, habit	colorless, block	colorless, block	colorless, block	yellow, block
Cryst size/mm	0.40 × 0.20 × 0.10	0.24 × 0.10 × 0.10	0.18 × 0.16 × 0.16	0.18 × 0.12 × 0.08
Temperature/K	243(2)	223(2)	223(2)	223(2)
Crystal system	triclinic	triclinic	triclinic	orthorhombic
Space group	$P\bar{1}$	$P\bar{1}$	$P\bar{1}$	*Pbcn*
a/Å	11.504(3)	11.8217(9)	11.0762(5)	31.2166(19)
b/Å	11.595(3)	11.8738(9)	12.6526(6)	11.1730(7)
c/Å	12.552(3)	12.7681(9)	13.6890(7)	17.026(1)
α/°	96.355(5)	69.492(2)	90.219(1)	90
β/°	99.264(5)	75.399(2)	106.606(1)	90
γ/°	98.275(5)	64.829(1)	97.676(1)	90
V/Å^3	1619.7(7)	1507.98(19)	1820.15(15)	5938.3(6)
Z	2	2	2	8
D_c/g cm^{-3}	1.398	1.693	1.499	1.680
Radiation used	Mo Kα	Mo Kα	Mo Kα	Mo Kα
μ/mm^{-1}	2.597	3.363	2.795	2.085
θ range/°	1.66–24.99	1.72–25.00	1.63–27.49	1.30–25.00
Reflection collected	16547	15898	24120	32991
Independent reflections	5687	5301	8345	5235
R(int)	0.0806	0.0557	0.0569	0.1100
Max., min. transmission	0.7812, 0.4231	0.7297, 0.4991	0.6633, 0.6331	0.8510, 0.7054
Final R indices [$I > 2\sigma(I)$]	$R_1 = 0.0821$, $wR_2 = 0.2327$	$R_1 = 0.0732$, $wR_2 = 0.1630$	$R_1 = 0.0562$, $wR_2 = 0.1463$	$R_1 = 0.0530$, $wR_2 = 0.1173$
R indices (all data)	$R_1 = 0.1055$, $wR_2 = 0.2451$	$R_1 = 0.0890$, $wR_2 = 0.1697$	$R_1 = 0.0904$, $wR_2 = 0.1614$	$R_1 = 0.0977$, $wR_2 = 0.1342$
Goodness-of-fit on F^2	1.062	1.215	1.044	1.020
Peak/hole/e Å^{-3}	2.224/–0.522	2.060/–0.902	1.013/–0.471	1.176/–1.277

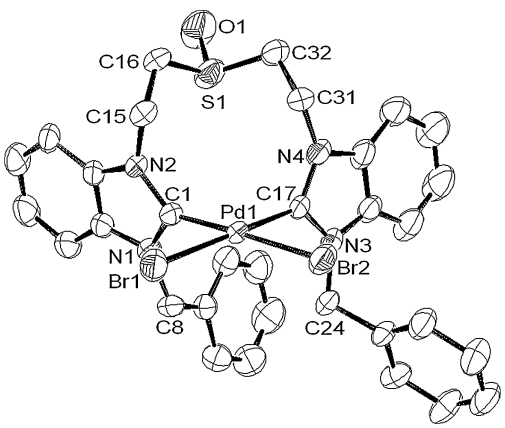

Fig. 3 Molecular structure of pseudo-pincer complex **2**·0.5DMF showing 50% probability ellipsoids; hydrogen atoms and the solvent molecule are omitted for clarity. Selected bond lengths (Å) and angles (°): Pd1–C1 1.991(6), Pd1–C17 1.987(5), Pd1–Br1 2.4765(7), Pd1–Br2 2.4649(7), N1–C1 1.340(7), N1–C8 1.472(7), N2–C1 1.360(6), N2–C15 1.457(7), N3–C17 1.355(7), N3–C24 1.450(7), N4–C17 1.365(7), N4–C31 1.467(7), S1–O1 1.490(5), S1–C16 1.790(6), S1–C32 1.817(7); C1–Pd1–Br1 84.28(15), C1–Pd1–C17 96.1(2), C17–Pd1–Br2 86.57(15), Br1–Pd1–Br2 93.03(3), C1–Pd1–Br2 177.24(15), C17–Pd1–Br1 179.25(17), N1–C1–N2 106.5(5), N3–C17–N4 105.7(5); PdC_2Br_2/NHC dihedral angle 84°, 81°; inter-NHC angle 76°.

donor. Disappointingly, the equimolar reaction of **B**·2HNO_3 with $Pd(OAc)_2$ in DMSO at 80 °C only led to substantial formation of Pd black.

It was anticipated that the lack of stabilizing anionic ligands was the cause for this decomposition. Indeed with the addition of 1 equiv of KBr, which can take up the fourth coordination site, the reaction proceeded smoothly and the desired product [PdBr(**B**-κ^3*CSC*)]NO_3 (**3**), could be isolated in a good yield of 68%. The solubility of complex **3** in common organic solvents is similar to that of **2**. Although the ESI mass spectrum shows a cationic base peak at $m/z = 689$ for the $[M - NO_3]^+$ complex cation, it does not provide sufficient evidence for the formation of **3**, since the same base peak has been observed for the $[M - Br]^+$ fragment of **1**. On the other hand, NMR spectroscopy reveals distinct differences. The coordination of the sulfur atom results in diastereotopy of the adjacent methylene protons, which resonance at 5.03 and 3.44 ppm as two broad pseudo-triplets. Furthermore, the carbenoid ^{13}C signals are observed downfield from those in **1** at 176.6 ppm, indicating a *trans* arrangement of the two benzimidazolin-2-ylidene moieties. However, this chemical shift difference is not as pronounced as in direct *cis-trans* isomers[9] as a consequence of the different overall Lewis acidity of neutral **1** and cationic **3**. Vapour diffusion of diethyl ether into a DMF solution afforded single crystals that were subjected to X-ray diffraction studies. Fig. 4 depicts the molecular structure of the first CSC-pincer complex bearing NHC ligands. As found in solution, pincer-type coordination forces the two carbene donors into a *trans*-arrangement incorporating the Pd(II) center into two six-membered rings. As anticipated, the fourth coordination site *trans* to the sulfur donor is taken up by a bromo ligand resulting in a square planar complex-cation, the charge of which is compensated by one NO_3^- counter-anion. Pincer formation also leads to a substantial decrease of the inter-NHC angle to 15°. The dihedral angles between the carbene ring planes and the PdC_2SBr-coordination plane also decrease to 47° and 61°, respectively. As a consequence of the *trans* arrangement, the Pd-C bonds of 2.033(6) and 2.000(6) Å have become elongated compared those in **1** and **2**. They are also similar to those reported for related CNC pincer

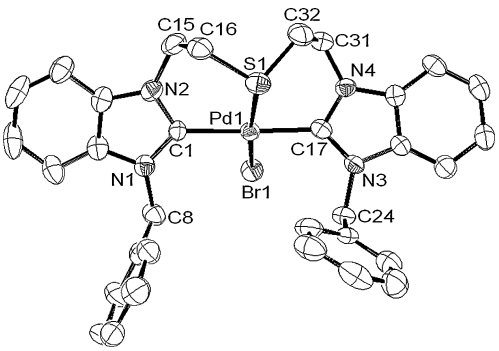

Fig. 4 Molecular structure of CSC-pincer complex **3** showing 50% probability ellipsoids; hydrogen atoms and the NO_3^- counter-anion are omitted for clarity. Selected bond lengths (Å) and angles (°): Pd1–C1 2.033(6), Pd1–C17 2.000(6), Pd1–S1 2.3078(18), Pd1–Br1 2.4341(8), N1–C1 1.361(8), N1–C8 1.468(7), N2–C1 1.356(7), N2–C15 1.472(8), N3–C17 1.347(7), N3–C24 1.472(8), N4–C31 1.461(7), N4–C17 1.345(8), S1–C16 1.800(7), S1–C32 1.825(7); C1–Pd1–Br1 93.59(18), C1–Pd1–S1 93.16(18), C17–Pd1–S1 84.46(17), C17–Pd1–Br1 88.66(17), C17–Pd1–C1 177.3(2), S1–Pd1–Br1 171.10(5), N1–C1–N2 105.2(5), N3–C17–N4 106.3(5); PdC_2SBr/NHC dihedral angle 47°, 61°; inter-NHC angle 15°.

complexes containing benzannulated carbene donors.[12,13] On the other hand, the Pd–Br bond of 2.4341(8) is shorter due to the smaller *trans*-influence of the sulfur donor. Finally, the Pd–S bond is comparable to that of a thioether-functionzed NHC complex reported earlier.[7]

Catalysis

The Mizoroki–Heck reaction of aryl bromides with *tert*-butyl acrylate in DMF was selected to test and compare the initial catalytic activities of the pseudo-pincer complexes **1** and **2** as well as the pincer-complex **3**. The results summarized in Table 1 demonstrate that all three complexes are suitable catalyst precursors leading to quantitative yields for a range of activated substrates (entries 1–13). The coupling of dibromo-pyridine is also successful giving quantitatively the doubly-coupled product (*E,E′*)-di-*tert*-butyl-3,3′-(pyridine-2,6-diyl)diacrylate (entries 13–15). The latter result is encouraging and demonstrates superior activities of benzimidazole-derived NHCs over a previously reported imidazole-based bis(carbene) system.[14] Surprisingly, the reaction with 1-bromo-4-chlorobenzene turned out to be rather sluggish resulting in only moderate yields (entries 16–18). The limitations of all three complexes finally become evident in the coupling of deactivated substrates, where poor to moderate yields were obtained (entries 19–24). A better performance has been reported for a similar lutidine-bridged CNC pincer.[12] Notably, a comparison did not reveal the superiority of any complex. It was observed that any of the three complexes can give rise to the best yield dependant on the substrate used (entries 17, 19, 24). However, as these differences are rather small, it can be anticipated that all three complexes decompose under the relatively harsh conditions to palladium nanoparticles of very similar size that do the catalytic work.

In a separate study, the influence of the catalyst loading on the Mizoroki–Heck coupling reaction catalyzed by the pincer complex **3** was investigated as well (Table 2). Here it was observed, that **3** could still give quantitative yield with a loading of as low as 10^{-3} mol% when the reaction time was extended to 48 h. This result is promising and indicates that the sulfur function in the bridge does not poison the active Pd(0) catalyst. However, further decrease of catalyst loading to 2×10^{-4} mol% and extension of the reaction time to 78 h results in a dramatic drop of yield to 36%, although a relatively high TON of 180 000 could be achieved. Again, these results are superior than those reported for complexes bearing COC-quasi-pincer[10] or CNC-pincer-type[15] carbene ligands derived from imidazole.

Conclusions

In summary, we have reported on the design of three new dibenzimidazolium salt precursors bearing thioether (**B**·2HBr, **B**·$2HNO_3$) and sulfoxide (**C**·2HBr) groups. Reaction of the dibromide salts with $Pd(OAc)_2$ under standard conditions afforded the pseudo-pincer complexes *cis*-[$PdBr_2$(**B**-κ^2C)] (**1**) and *cis*-[$PdBr_2$(**C**-κ^2C)] (**2**), in which the sulfur donors remain uncoordinated, but potentially hemilabile. Using an improved protocol involving palladation of **B**·$2HNO_3$ in the presence of 1 equiv of KBr, the first CSC pincer complex [PdBr(**B**-κ^3CSC)]NO_3 (**3**) could be isolated in a good yield. All new complexes have been fully characterized, and a first catalytic investigation showed that all complexes are highly active only in the Mizoroki–Heck coupling of activated aryl bromides, whereas deactivated substrates gave moderate to poor results. More importantly, these results demonstrate that the sulfur function did not poison the active catalyst and research in our lab is currently on-going to extend the promising coordination chemistry of these new ligands to different transition metals in search for other catalytic applications.

Experimental

General considerations

Unless otherwise noted all operations were performed without taking precautions to exclude air and moisture. All solvents and chemicals were used as received without any further treatment if not noted otherwise. 1-Benzylbenzimidazole was prepared according to a previously reported method.[16] ^1H and ^{13}C NMR spectra were recorded on a Bruker ACF 300 spectrometer or AMX 500 spectrophotometer and the chemical shifts (δ) were internally referenced by the residual solvent signals relative to tetramethylsilane (^1H, ^{13}C). ESI Mass spectra were measured using a Finnigan MAT LCQ spectrometer. Elemental analyses were performed on a Perkin-Elmer PE 2400 elemental analyzer at the Department of Chemistry, National University of Singapore.

Syntheses

1-Benzyl-3-(2-bromoethyl)-benzimidazolium bromide (A). A mixture of 1-benzylbenzimidazole (1.458 g, 7 mmol) and 1,2-dibromoethane (7 ml) was heated at 85 °C overnight. After removing the volatiles *in vacuo*, CH_2Cl_2 (50 ml) was added to the residue and the resulting suspension was filtered over Celite. The remaining solid was washed with CH_2Cl_2 (4 × 20 ml) and the solvent of the filtrate was removed *in vacuo* to give a white solid (2.550 g, 6.44 mmol, 92%). ^1H NMR (300 MHz, DMSO-d_6): δ 10.12 (s, 1 H, NCHN), 8.19 (dd, 1 H, Ar-H), 8.00 (dd, 1 H, Ar-H), 7.69 (m, 2 H, Ar-H), 7.51 (dd, 2 H, Ar-H), 7.41 (m,

3 H, Ar-H), 5.85 (s, 2 H, NCH_2Ph), 5.03 (t, ^3J(H,H) = 5.8 Hz, 2 H, NCH_2), 4.08 (t, ^3J(H,H) = 5.8 Hz, 2 H, CH_2Br). $^{13}C\{^1H\}$ NMR (75.47 MHz, DMSO-d_6): 143.0 (s, NCHN), 133.9, 131.0, 130.7, 129.0, 128.8, 128.2, 126.9, 114.1, 114.0 (s, Ar-C), 49.9 (s, NCH_2Ph), 48.1 (s, NCH_2), 31.1 (s, CH_2Br). MS (ESI): m/z = 316 $[M - Br]^+$.

B·2HBr. A mixture of salt **A** (792 mg, 2 mmol) and $Na_2S{\cdot}9H_2O$ (240 mg, 1 mmol) in CH_3CN was stirred at ambient temperature for 48 h. After removing the volatiles *in vacuo*, CH_2Cl_2 (3 × 20 ml) was added to the residue and the resulting suspension was filtered over Celite. The remaining solid left in the flask and on the Celite was dissolved in methanol. The product was crystallized from methanol (0.579 g, 0.87 mmol, 87%). ^1H NMR (300 MHz, DMSO-d_6): δ 10.39 (s, 2 H, NCHN), 8.20 (dd, 2 H, Ar-H), 7.98 (dd, 2 H, Ar-H), 7.65 (m, 4 H, Ar-H), 7.55 (d, 4 H, Ar-H), 7.37 (m, 6 H, Ar-H), 5.87 (s, 4 H, NCH_2Ph), 4.87 (t, ^3J(H,H) = 6.3 Hz, 4 H, NCH_2), 3.29 (t, ^3J(H,H) = 6.3 Hz, 4 H, CH_2S). $^{13}C\{^1H\}$ NMR (75.47 MHz, DMSO-d_6): 142.9 (s, NCHN), 134.0, 131.1, 130.6, 128.9, 128.7, 128.3, 126.74, 126.71, 114.2, 113.9 (s, Ar-C), 49.8 (s, NCH_2Ph), 46.0 (s, NCH_2), 29.4 (s, CH_2S). MS (ESI): m/z = 585 $[M - Br]^+$, 252 $[M - 2Br]^{2+}$.

B·2HNO$_3$. A mixture of salt **B**·2HBr (266 mg, 0.4 mmol) and $AgNO_3$ (136 mg, 0.8 mmol) in methanol (20 ml) was stirred at ambient temperature overnight. The resulting suspension was filtered from the precipitated AgBr over Celite and the solvent was removed *in vacuo* to give the product as a white powder (207 mg, 0.329 mmol, 83%). ^1H NMR (300 MHz, DMSO-d_6): δ 10.15 (s, 2 H, NCHN), 8.16 (dd, 2 H, Ar-H), 7.97 (dd, 2 H, Ar-H), 7.66 (m, 4 H, Ar-H), 7.52 (dd, 4 H, Ar-H), 7.38 (m, 6 H, Ar-H), 5.83 (s, 4 H, NCH_2Ph), 4.83 (t, ^3J(H,H) = 6.5 Hz, 4 H, NCH_2), 3.24 (t, ^3J(H,H) = 6.5 Hz, 4 H, CH_2S). $^{13}C\{^1H\}$ NMR (75.47 MHz, DMSO-d_6): 142.9 (s, NCHN), 134.0, 131.2, 130.7, 129.0, 128.7, 128.2, 126.8, 126.7, 114.1, 113.9 (s, Ar-C), 49.9 (s, NCH_2Ph), 46.0 (s, NCH_2), 29.4 (s, CH_2S). MS (ESI): m/z = 566 $[M - NO_3]^+$, 252 $[M - 2NO_3]^{2+}$.

C·2HBr. A mixture of salt **B**·2HBr (200 mg, 0.3 mmol) and 35% H_2O_2 (78 μL, 0.9 mmol) in acetic acid (5 ml) was stirred at ambient temperature overnight. After removing the volatiles *in vacuo*, the residue was washed with THF (3 × 20 ml) to give an off-white powder (185 mg, 0.27 mmol, 91%). ^1H NMR (300 MHz, DMSO-d_6): δ 10.15 (s, 2 H, NCHN), 8.14 (dd, 2 H, Ar-H), 7.95 (dd, 2 H, Ar-H), 7.67 (m, 4 H, Ar-H), 7.51 (m, 4 H, Ar-H), 7.37 (m, 6 H, Ar-H), 5.82 (s, 4 H, NCH_2Ph), 5.05 (br t, 4 H, NCH_2), 3.70 (dt, ^2J(H,H) = 13.6 Hz, ^3J(H,H) = 6.0 Hz, 2 H, C*H*HS), 3.56 (dt, ^2J(H,H) = 13.6 Hz, ^3J(H,H) = 6.0 Hz, 2 H, CH*H*S). $^{13}C\{^1H\}$ NMR (75.47 MHz, DMSO-d_6): 143.1 (s, NCHN), 133.8, 131.2, 130.6, 128.9, 128.6, 128.3, 128.0, 126.7, 114.0, 113.97 (s, Ar-C), 49.9 (s, NCH_2Ph), 49.2 (s, NCH_2), 41.3 (s, CH_2S). MS (ESI): m/z = 602 $[M - Br]^+$, 260 $[M - 2Br]^{2+}$.

***cis*-[PdBr$_2$(B-κ^2*C*)] (1).** A mixture of salt **B**·2HBr (200 mg, 0.3 mmol) and $Pd(OAc)_2$ (67 mg, 0.3 mmol) in DMSO (5 ml) was stirred at 80 °C overnight. The resulting mixture was filtered over Celite, and the solvent of the filtrate was removed by vacuum distillation. The resulting residue was washed with H_2O (3 × 20 ml). The residue was then dissolved in CH_2Cl_2 and filtered over Celite. The filtrate was dried under vacuum and the remaining solid was washed with THF to obtain the desired product as a yellow solid (120 mg, 0.13 mmol, 42%). ^1H NMR (500 MHz, DMSO-d_6): δ 7.75 (d, 2 H, Ar-H), 7.26 (m, 4 H, Ar-H), 7.19 (m, 4 H, Ar-H), 7.12 (m, 6 H, Ar-H), 6.86 (d, 2 H, Ar-H), 6.35 (d, ^2J(H,H) = 16.4 Hz, 2 H, NC*H*HPh), 5.84 (m, 2 H, NC*H*H), 5.30 (d, ^2J(H,H) = 16.4 Hz, 2 H, NCH*H*Ph), 4.85 (d, ^2J(H,H) = 13.9 Hz, 2 H, NCH*H*), 3.50 (m, 4 H, CH_2S). $^{13}C\{^1H\}$ NMR (125.77 MHz, DMSO-d_6): 175.2 (s, NCN), 135.2, 133.6, 133.2, 128.4, 127.8, 126.9, 123.3, 123.2, 111.9, 111.7 (s, Ar-H), 51.5 (s, NCH_2Ph), 50.3 (s, NCH_2), 33.0 (s, CH_2S). Anal. Calc. for $C_{32}H_{30}Br_2N_4PdS$: C, 49.99; H, 3.93; N, 7.29. Found: C, 49.94; H, 3.92; N, 7.25%. MS (ESI): m/z = 689 $[M - Br]^+$.

***cis*-[PdBr$_2$(C-κ^2*C*)] (2).** A mixture of salt **C**·2HBr (205 mg, 0.3 mmol) and $Pd(OAc)_2$ (67 mg, 0.3 mmol) in DMSO (5 ml) was stirred at 80 °C overnight. The resulting mixture was filtered over Celite, and the solvent of the filtrate was removed by vacuum distillation. The resulting residue was washed with H_2O (3 × 20 ml) and redissolved in CH_2Cl_2. Slow evaporation of CH_2Cl_2 solution afforded the product as a white solid (120 mg, 0.15 mmol, 51%). ^1H NMR (500 MHz, DMSO-d_6): δ 7.93 (d, 2 H, Ar-H), 7.35 (m, 2 H, Ar-H), 7.24 (m, 2 H, Ar-H), 7.18 (m, 6 H, Ar-H), 7.07 (m, 4 H, Ar-H), 6.90 (d, 2 H, Ar-H), 6.26 (d, ^2J(H,H) = 16.4 Hz, 2 H, NC*H*HPh), 5.99 (m, 2 H, NC*H*H), 5.35 (d, ^2J(H,H) = 16.4 Hz, 2 H, NCH*H*Ph), 4.82 (m, 2 H, NCH*H*), 4.31 (m, 2 H, CH*H*S), 3.71 (m, 2 H, C*H*HS). $^{13}C\{^1H\}$ NMR (125.77 MHz, DMSO-d_6): 173.8 (s, NCN), 134.8, 133.7, 133.5, 128.4, 127.8, 126.8, 123.8, 123.7, 112.1, 111.8 (s, Ar-H), 51.8 (s, NCH_2Ph), 51.2 (s, NCH_2), 43.5 (s, CH_2S). Anal. Calc. for $C_{32}H_{30}Br_2N_4OPdS$: C, 48.97; H, 3.85; N, 7.14. Found: C, 48.87; H, 4.05; N, 7.50%. MS (ESI): m/z = 705 $[M - Br]^+$.

[PdBr(B-κ^3*CSC*)]NO$_3$ (3). A mixture of salt **B**·2HNO$_3$ (198 mg, 0.32 mmol), KBr (37.5 mg, 0.32 mmol) and $Pd(OAc)_2$ (71 mg, 0.32 mmol) in DMSO (5 ml) was stirred at 80 °C overnight. The resulting mixture was filtered over Celite, and the solvent of the filtrate was removed by vacuum distillation. The resulting residue was washed with H_2O (3 × 20 ml), subsequently with CH_2Cl_2 (3 × 20 ml) and dried under vacuum to afford the product as a yellow powder (162 mg, 0.215 mmol, 68%). ^1H NMR (500 MHz, DMSO-d_6): δ 8.03 (d, 2 H, Ar-H), 7.70(d, 2 H, Ar-H), 7.47 (m, 2 H, Ar-H), 7.42 (m, 2 H, Ar-H), 7.35 (m, 4 H, Ar-H), 7.20 (m, 6 H, Ar-H), 6.36 (d, ^2J(H,H) = 15.8 Hz, 2 H, NC*H*HPh), 5.85 (d, ^2J(H,H) = 15.8 Hz, 2 H, NCH*H*Ph), 5.37 (d, ^2J(H,H) = 13.9 Hz, 2 H, NC*H*H), 5.03 (ps t, ^2J(H,H) = 12.6 Hz, 2 H, C*H*HS), 3.73 (d, ^2J(H,H) = 13.9 Hz, 2 H, NCH*H*), 3.44 (ps t, ^2J(H,H) = 12.6 Hz, 2 H, CH*H*S). $^{13}C\{^1H\}$ NMR (75.47 MHz, DMSO-d_6): 176.6 (s, NCN), 136.4, 134.2, 133.6, 129.0, 128.2, 127.7, 124.6, 124.5, 112.5, 112.4 (s, Ar-H), 51.4 (s, NCH_2Ph), 49.0 (s, NCH_2), the signal for CH_2S overlaps with residual signals of DMSO-d_6. Anal. Calc. for $C_{32}H_{30}BrN_5O_3PdS$: C, 51.18; H, 4.03; N, 9.33. Found: C, 50.81; H, 4.30; N, 9.00%. MS (ESI): m/z = 689 $[M - NO_3]^+$.

Mizoroki–Heck catalysis

In a typical run, a reaction tube was charged with a mixture of aryl halide (1.0 mmol for monohalides, 0.5 mmol for dihalides), anhydrous sodium acetate (1.5 mmol), *tert*-butyl acrylate (1.4 mmol), catalyst (0.01 mmol) and DMF (3 ml). The reaction was stirred and heated at 120 °C for 24 h. After the mixture was cooled to the ambient temperature, dichloromethane (10 ml) was added. The

organic layer was then washed with water (6 × 8 ml) and dried over Na_2SO_4. The solvent was allowed to evaporate and the residue was analyzed by ^{1}H NMR spectroscopy.

X-Ray diffraction studies

Diffraction data were collected with a Bruker AXS SMART APEX diffractometer, using Mo Kα radiation at 223(2) (**1-3**) or 243(2) K (**B**·2HBr), with the SMART suite of Programs.[17] Data were processed and corrected for Lorentz and polarisation effects with SAINT,[18] and for absorption effect with SADABS.[19] Structural solution and refinement were carried out with the SHELXTL suite of programs.[20] The structure was solved by direct methods to locate the heavy atoms, followed by difference maps for the light, non-hydrogen atoms. All hydrogen atoms were put at calculated positions. All non-hydrogen atoms were generally given anisotropic displacement parameters in the final model. A summary of the most important crystallographic data is given in the Table 3. CCDC reference numbers 728535 (**B**·2HBr·0.8H_2O), 728532 (**1**), 728533 (**2**·0.5DMF) and 728534 (**3**).†

Acknowledgements

We thank the National University of Singapore for financial support (Grant No. R 143-000-327-133) and the CMMAC staff of our department for technical assistance.

Notes and references

1 For a recent review, see: F. E. Hahn and M. C. Jahnke, *Angew. Chem., Int. Ed.*, 2008, **47**, 3122.
2 For a recent review, see: A. T. Normand and K. J. Cavell, *Eur. J. Inorg. Chem.*, 2008, 2781.
3 (*a*) M. Albrecht and G. van Koten, *Angew. Chem., Int. Ed.*, 2001, **40**, 3751; (*b*) I. P. Beletskaya and A. V. Cheprakov, *Chem. Rev.*, 2000, **100**, 3009; (*c*) D. Morales-Morales and C. M. Jensen, *The Chemistry of Pincer Compounds*, Elsevier, Amsterdam, Netherlands, 2007.
4 For a recent review, see: D. Pugh and A. A. Danopoulos, *Coord. Chem. Rev.*, 2007, **251**, 610.
5 D. Sellmann, C. Allmann, F. Heinemann, F. Koch and J. Sutter, *J. Organomet. Chem.*, 1997, **541**, 291.
6 N. Matsumura, J. Kawano, N. Fukunishi, H. Inoue, M. Yasui and F. Iwasaki, *J. Am. Chem. Soc.*, 1995, **117**, 3623.
7 H. V. Huynh, C. H. Yeo and G. K. Tan, *Chem. Commun.*, 2006, 3833.
8 H. V. Huynh and Y. X. Chew, *Inorg. Chim. Acta*, 2009, DOI: 10.1016/j.ica.2009.02.035, in press.
9 H. V. Huynh, J. H. H. Ho, T. C. Neo and L. L. Koh, *J. Organomet. Chem.*, 2005, **690**, 3854.
10 D. J. Nielsen, K. J. Cavell, B. W. Skelton and A. H. White, *Organometallics*, 2006, **25**, 4850.
11 C. Marshall, M. F. Ward and W. T. A. Harrison, *Tetrahedron Lett.*, 2004, **45**, 5703.
12 F. E. Hahn, M. C. Jahnke, V. Gomez-Benitez, D. Morales-Morales and T. Pape, *Organometallics*, 2005, **24**, 6458.
13 D. H. Brown, G. L. Nealon, P. V. Simpson, B. W. Skelton and Z. Wang, *Organometallics*, 2009, **28**, 1965.
14 H. V. Huynh and J. Wu, *J. Organomet. Chem.*, 2009, **694**, 323.
15 D. J. Nielsen, K. J. Cavell, B. W. Skelton and A. H. White, *Inorg. Chim. Acta*, 2002, **327**, 116.
16 H. V. Huynh, L. R. Wong and P. S. Ng, *Organometallics*, 2008, **27**, 2231.
17 *SMART version 5.628*, Bruker AXS Inc., Madison, Wisconsin, USA, 2001.
18 *SAINT+ version 6.22a*, Bruker AXS Inc., Madison, Wisconsin, USA, 2001.
19 G. W. Sheldrick, *SADABS version 2.10*, University of Göttingen, 2001.
20 *SHELXTL version 6.14*, Bruker AXS Inc., Madison, Wisconsin, USA, 2000.

